Photodiagnosis and Photodynamic Therapy 34 (2021) 102309

Contents lists available at ScienceDirect

Photodiagnosis and Photodynamic Therapy

journal homepage: www.elsevier.com/locate/pdpdt

The sustaining of fluorescence in photodynamic diagnosis after the administration of 5-aminolevulinic acid in carcinogen-induced bladder cancer orthotopic rat model and urothelial cancer cell lines

Takuya Owari [a,1], Takashi Iwamoto [a,1], Satoshi Anai [a], Makito Miyake [a], Yasushi Nakai [a], Shunta Hori [a], Takeshi Hara [b], Takuya Ishii [b], Urara Ota [b], Kazumasa Torimoto [a], Hiroki Kuniyasu [c], Tomomi Fujii [d], Nobumichi Tanaka [a], Kiyohide Fujimoto [a,*]

[a] Department of Urology, Nara Medical University, Kashihara, Nara, Japan
[b] SBI Pharmaceuticals Co., Ltd., Minato-ku, Tokyo, Japan
[c] Department of Molecular Pathology, Nara Medical University, Kashihara, Nara, Japan
[d] Department of Pathology, Nara Medical University, Kashihara, Nara, Japan

ARTICLE INFO

Keywords:
5-Aminolevulic acid hydrochloride
Bladder cancer
Photodynamic diagnosis
Protoporphyrin IX
Carcinogen-induced bladder cancer orthotopic rat model

ABSTRACT

Background: The administration of 5-aminolevulic acid hydrochloride (5-ALA·HCl) 3 h (range: 2–4 h) before photodynamic diagnosis (PDD) is recommended for detecting bladder tumors. However, there is insufficient evidence on the time duration for the fluorescence of PDD after oral administration of 5-ALA. We investigated the sustainability of the photodynamic effect and protoporphyrinIX (PpIX) after 5-ALA administration in a carcinogen-induced bladder tumor rat model and bladder cancer cell lines.

Methods: The carcinogen-induced bladder tumor orthotopic rat model was established by the administration of N-butyl-N-(4-hydroxybutyl) nitrosamine.

Results: Red fluorescence was visible 2–8 h after the oral administration of 5-ALA in the carcinogen-induced bladder tumor rat model. Plasma and intratissue PpIX (nM) progressed to a higher level at 2 h and remained almost constant 2–8 h after oral administration of 5-ALA. The peak fluorescence intensity of PpIX was observed 3–4 h after the administration of 5-ALA in bladder cancer cell lines. The accumulated PpIX remained for 4 h after the removal of 5-ALA in UMUC3 cells. It was not clearly visible 3 h after the removal of 5-ALA in MGHU3 and T24 cells. The expression level of ferrochelatase was significantly lower in UMUC3 cells than in other cells. Our findings suggest that 5-ALA-assisted PDD (ALA-PDD) can aid in detecting non-muscle-invasive bladder cancer 2–8 h after 5-ALA administration.

Conclusion: Urologists might not be required to make excess effort to start ALA-PDD-assisted transurethral resection of bladder tumor after the administration of 5-ALA.

1. Introduction

Bladder cancer is the ninth most common malignancy worldwide. It is estimated that 430,000 new cases were diagnosed in 2012 and is the most common malignancy involving the urinary system [1,2]. Approximately 75–80 % of bladder cancer patients present with non-muscle-invasive bladder cancer (NMIBC), and Ta (non-muscle-invasive papillary carcinoma) is the most common phenotype of NMIBC (60 %), whereas T1 (invasion to the lamina propria) and carcinoma *in situ* (CIS) account for 30 % and 10 % of all tumors, respectively [3,4]. Transurethral resection of bladder tumor (TURBT) is the most important initial step in therapeutic management and disease diagnosis (*e.g.*, tumor grade, invasion into the muscle, or presence of concomitant CIS). There is consensus on the importance of resection of all visible bladder tumors at the initial TURBT to determine the optimal management for reducing the risk of recurrence and progression [5]. However, several studies have revealed that residual tumors, which are associated with early recurrence, are frequently observed (52–76 %),

* Corresponding author at: Department of Urology, Nara Medical University, 840 Shijo-cho, Kashihara, Nara, 634-8521, Japan.
E-mail address: kiyokun@naramed-u.ac.jp (K. Fujimoto).
[1] These authors equally contribution to this study.

https://doi.org/10.1016/j.pdpdt.2021.102309
Received 8 March 2021; Received in revised form 12 April 2021; Accepted 19 April 2021
Available online 24 April 2021

and the rate of down-staging ranges from 9.4%–29% [6–8] during the initial TURBT. Moreover, flat lesions such as CIS are difficult to detect by cystoscopy. Currently, to reduce the frequency of the residual tumor and improve the detection of flat lesions, photodynamic diagnosis-assisted TURBT using 5-aminolevulic acid hydrochloride (5-ALA·HCl) or hexaminolevulinic acid (HAL) is developed for the initial management of NMIBC.

5-ALA, a precursor of heme biosynthesis, is a naturally occurring amino acid that is synthesized from succinyl coenzyme A and glycine. Exogenously administered 5-ALA can be enzymatically converted into protoporphyrin IX (PpIX) the mitochondria through the heme biosynthetic pathway. Ferrochelatase (FECH) catalyzes the insertion of ferrous iron into PpIX, thereby converting it into heme at the final step in the heme biosynthesis pathway. PpIX is preferentially accumulated in the mitochondria of cancer cells. One of the reasons for this accumulation might be the inactivation of FECH in cancer cells due to insufficient electron supply from the tricarboxylic acid cycle (Warburg effect) [9]. Particularly, bladder cancer cells show 9- to 16-fold accumulation of PpIX compared to that in normal urothelial cells [10]. We previously showed that downregulated expression of FECH is associated with increased accumulation of PpIX in urothelial bladder cancer [11,12].

PpIX, a key molecule, is the photosensitizer during the photodynamic diagnosis mediated by 5-ALA (ALA-PDD). Intracellular PpIX is visible as red fluorescence at an excitation wavelength of approximately 400 nm and a peak emission wavelength of 635 nm [13]. In 1994, for the first time, Kriegmair et al. described ALA-PDD as a promising tool for detecting bladder cancer, which was difficult to visualize by standard cystoscopy [14]. Recently, the European Association of Urology (EAU) guidelines in 2020 (on web) [15] and the Japanese Urological Association (JUA) guidelines in 2019 [16] strongly recommended ALA-PDD-assisted TURBT for the management of NMIBC.

In Japan, multicenter phase II/III and phase III studies demonstrated that the sensitivity of PDD with 20 mg/kg of oral administration of 5-ALA·HCl 3 h (range: 2–4 h) before TURBT was higher than that of conventional white-color light source endoscopy (75.8 % *vs.* 47.6 % and 79.6 % *vs.* 54.1 %, respectively) [17,18]. Based on these findings, ALA-PDD-assisted TURBT was approved by the Japanese Pharmaceuticals and Medical Devices Agency in 2017, and oral administration of 5-ALA·HCl 3 h (range: 2–4 h) before TURBT is recommended. However, there is insufficient evidence for the time duration of fluorescence of PDD after oral administration of 5-ALA·HCl for detecting bladder cancer. We aimed to evaluate the sustainability of the photodynamic effect of 5-ALA on ALA-PDD-assisted TURBT and confirmed whether the fluorescence in ALA-PDD could be detected when time had unexpectedly passed after the administration of 5-ALA.We performed time-dependent monitoring of the fluorescence intensity and accumulation of PpIX after exogenous administration of 5-ALA using three different phenotypes of bladder cancer cell lines and carcinogen-induced bladder cancer orthotopic rat model established by the administration of N-butyl-N-(4-hydroxybutyl) nitrosamine (BBN).

2. Materials and methods

2.1. Cell culture, reagents, and treatment

UMUC-3, MGHU-3, and T24 human bladder cancer cell lines were purchased from American Type Culture Center (ATCC; Manassas, VA, USA). Cells were cultured in Dulbecco's modified Eagle's medium (DMEM), supplemented with 10 % fetal bovine serum (FBS) and 2% penicillin/streptomycin at t 37 °C in a humidified 5%5-ALA·HCl was supplied by SBI Pharmaceuticals Co., Ltd. (Tokyo, Japan).

2.2. Accumulated intracellular protoporphyrin IX quantification technique in cell lines

The quantification of accumulated intracellular PpIX in 1 mM of 5-ALA administered cells was performed using fluorescence imaging. UMUC-3, MGHU-3, and T24 cells at density of 1.0×10^5 cells/well were seeded in cell culture dish (35 × 10 mm) overnight and incubated with 1 mM of 5-ALA for different time (0, 1, 2, 3, 4, 6, and 8 h). Subsequently, the medium was washed with phosphate-buffered saline (PBS) twice and replaced with 5-ALA-free new medium. Finally, accumulated PpIX was immediately observed. We also observed PpIX at different time-points (0, 1, 2, 3, and 4 h) after incubation with 5-ALA for 4 h, and the medium was washed with PBS twice and replaced with an ALA-free new medium. Fluorescence imaging of PpIX was visualized under a fluorescence microscope (BZ-X710, KEYENCE, Osaka, Japan) with a specific filter (405 nm excitation, 630 nm emission) (M Square, Fukuoka, Japan). To evaluate the location of accumulated PpIX, the mitochondria were labelled with MitoGreen (PromoCell, Heidelburg, Germany). The fluorescence intensity of 5-ALA-administered cells was analyzed using BZ-X analysis software (KEYENCE, Osaka, Japan).

2.3. Immunoblot analysis

Whole-cell protein was extracted from UMUC-3, MGHU-3, and T24 cells using RIPA buffer with protease inhibitor cocktail (Nacalai Tesque, Kyoto, Japan). The extracted proteins (20 μg) were subjected to immunoblot analysis using sodium dodecyl sulfate-polyacrylamide gel electrophoresis (12 %), followed by electrotransfer using Mini-Protean TGX Gel (Bio-Rad, Laboratories, Hercules, CA, USA) and transferred onto a polyvinylidene fluoride membrane. After blocking with Tris-buffered saline with Tween 20 (TBS-T) containing 5% skimmed milk, the membranes were incubated with primary antibodies diluted in TBS-T with 5% skimmed milk, overnight at 4 °C. The primary antibodies for ferrochelatase (A-3) (sc-377377, mouse monoclonal, 1:500) and β-actin (AC-15) (sc-69879, mouse monoclonal, 1;10,000) were purchased from Santa Cruz Biotechnologies (Dallas, CA, USA). The membranes were incubated with horseradish peroxidase (HRP)-conjugated secondary antibodies for 1 h at room temperature. The immune complexes were visualized using the ChemiDoc™imaging system (Bio-Rad Laboratories, Hercules, CA, USA).

2.4. Quantitative real-time reverse transcription-polymerase chain reaction (RT-PCR)

Total RNA was extracted from UMUC3, MGHU3, and T24 cells using TRIzol reagent (Thermo Fisher Scientific, Massachusetts, USA). cDNA was synthesized from mRNA (1 μg) using a High-Capacity cDNA Reverse Transcription Kit (Thermo Fisher Scientific, Massachusetts, USA). The primer sequences used for amplification were human FECH (forward, 5′-AGCACTATTGACAGGTGGCC; reverse, 5′-AGGATATGGGTCGCCTCT GT) and human β-actin (forward, 5′-GGACTTCGAGCAAGAGATGG; reverse, 5′-AGCACTGTGTTGGCGTACAG). For quantitative mRNA expression levels, β-actin was used as the internal control. RT-PCR was performed for FECH and β-actin using SYBR green (TB Green ® premix Ex Taq; Takara Bio Inc., Shiga, Japan). The conditions for RT-PCR were 30 s at 95 °C and 40 cycles at 95 °C for 5 s and at 60 °C for 30 s, as recommended by the manufacturer. Fold changes in mRNA levels were calculated after normalization with β-actin using the comparative Ct method.

2.5. Carcinogen-induced rat model

This animal study was approved by the Committee on Animal Research of Nara Medical University (Approval number:12670). All animal experiments were conducted in accordance with the Guidelines for Welfare of Animals in Experimental Neoplasia. Forty-four specific pathogen-free 5-week-old male Fischer344/Jcl rats were purchased from CLEA Japan (Tokyo, Japan). BBN has been used as a representative carcinogen of urothelial bladder tumors, and we established a carcinogen-induced bladder tumor-bearing rat model using a modified

previously reported technique [19,20]. We orally administered BBN at a concentration of 0.05 % diluted with drinking water for 20 weeks. Of the 44 rats, 2 did not receive BBN (negative control) and 42 rats received BBN (carcinogen-induced bladder tumor rat model).

2.6. Photodynamic diagnosis mediated by 5-aminolevulinic acid (ALA-PDD)

ALA-PDD was performed 10 weeks after the administration of BBN for 20 weeks. Forty-two carcinogen-induced bladder tumor rats were divided into 7 groups (n = 6); ALA-PDD was performed at 0, 1, 2, 3, 4, 6, and 8 h after the administration of 5-ALA. 5-ALA·HCl (200 mg/kg) was orally administered under isoflurane anesthesia. After the administration of 5-ALA·HCl at different time-points, the rats were immediately humanely euthanized, and bladder tissues and blood samples were collected. The collected bladder tissues were cut into two pieces. One half of the collected urinary bladder was fixed in 10 % paraformaldehyde for 24 h and embedded in paraffin. Another part of the collected bladder tissue was immediately used for ALA-PDD. We used D-Light C PDD system (KARL STORZ SE & CO., Tuttlingen, Germany), image1 S™HX-FI camera system (KARL STORZ SE & CO., Tuttlingen, Germany), and rigid cystoscopy for ALA-PDD. We performed ALA-PDD in a box covered with a black film to avoid photobleaching.

2.7. Fluorescence intensity measurement

We analyzed fluorescence intensity of ALA-PDD for 6 samples in each group. In 6 h group, we analyzed 5 samples because we lost one sample image for analysis. Fluorescence intensity of ALA-PDD was analyzed using ImageJ software according to a previously reported technique [21]. First, we adjusted the brightness and contrast of the ALA-PDD images. The images were split into RGB images, and R images were analyzed. Red-color fluorescence-positive regions were set as the regions of interest. We measured the area and the mean gray value, which is the average fluorescence intensity using the region of interest (ROI) manager.

2.8. Plasma and tissue PpIX concentration and plasma 5-ALA concentration

We analyzed 5-ALA and PpIX concentrations for 6 blood plasma and tissues in each group. To evaluate plasma PpIX, 5-ALA, and intratissue PpIX concentrations, we performed high-performance liquid chromatography (HPLC) using a modified previously reported technique [22,23]. Tissue samples were homogenized using T-10 basic ULTRA-TURRAX (IKA, Osaka, Japan). For the evaluation of PpIX concentration, 0.1 mL of plasma or homogenized tissue samples were mixed with 0.01 mL of 50 % v/v acetic acid and 0.3 mL of N, N-dimethylformamide-2-propanol (DMF-IPA) solution (100:1 by volume), and these solutions were centrifuged for 5 min (4℃, 14,000 rpm). DMF-IPA solution (150 μL) was added to the pellet, and the solutions were centrifuged for 5 min at 4 °C and 14,000 rpm. The collected supernatant was analyzed by HPLC using the Alliance HPLC System (Waters, MA, USA) and CAPCELL PAK C18 UG120 (inner diameter, 4.6 mm; length, 150 mm; particle size, 5 μm) (OSAKA SODA, Osaka, Japan). We used acetonitrile-10 mM tetrabutylammonium hydroxide (pH 7.5) solution (7:3 by volume) as the eluent (flow rate: 1.0 mL/min) and fluorescence (Ex, 400 nm; Em, 630 nm) was detected. Intratissue PpIX concentration was normalized to the total tissue protein concentration. Tissue protein concentration was measured using a protein assay dye reagent concentration (Bio-Rad Laboratories, Hercules, CA, USA).

For the evaluation of plasma 5-ALA concentration, 0.1 mL of plasma was mixed with 0.04 mL of 25 % w/v trichloroacetic acid solution, and these solutions were centrifuged for 10 min (4 °C, 14,000 rpm). Next, 0.01 mL of the collected supernatant was mixed with 0.24 mL of Milli-Q water, 0.25 mL of 200 mM acetic acidsodium acetate buffer (pH 3.8), 1.25 mL of solution A (68.4 mM sodium chloride containing 15 % v/v acetylacetone and 10 % v/v ethanol), and 0.25 mL of solution B (3.3 % w/w formaldehyde). These reaction mixtures were transferred into boiling water for 15 min, followed by immediate transfer to ice-cold water. Finally, they were analyzed by HPLC using Agilent1260 Infinity LC (Agilent Technologies, Santa Clara, CA, USA) and ZORBAX Eclipse Plus C18 Rapid Resolution HT (inner diameter: 4.6 mm, length: 50 mm, particle size: 1.8 μm) (Agilent Technologies, Santa Clara, CA, USA). We used 2.5 % acetic acid-methanol (6:4 by volume) as the eluent (flow rate: 0.5 mL/min) and fluorescence (Ex, 363 nm; Em, 473 nm) was detected.

2.9. Statistical analysis

Statistically significant differences were compared using two-tailed Student's *t*-test or one-way analysis of variance using GraphPad Prism 7.00 (GraphPad Software, San Diego, CA, USA). Statistical significance was set at $p < 0.05$.

3. Results

3.1. Photodynamic fluorescence after oral 5-aminolevulinic acid administration in carcinogen-induced bladder cancer orthotopic rat model

To evaluate the sustainability of PDD effect after oral 5-ALA administration *in vivo*, we performed ALA-PDD at 0, 1, 2, 3, 4, 6, and 8 h (n = 6; each group) after the oral administration of 5-ALA in a carcinogen-induced bladder cancer orthotopic rat model established by BBN administration (Fig. 1A). We orally administered BBN (a carcinogen) at a concentration of 0.05 % diluted with drinking water for 20 weeks according to a modified previously reported technique [19]. BBN-induced bladder tumors in rats have papillary and non-muscle-invasive characteristics [20]. The pathological characteristics of the 44 rats are shown in Table 1. Of the 42 rats with BBN administration, 41 had urothelial bladder tumors and 1 had no tumor (1 h-5). Of the 41 rats with urothelial bladder tumors, 38 (93 %) had non-muscle-invasive bladder tumors (Ta, 34 rats; T1, 4 rats) and 3 (7%) had muscle-invasive bladder tumors. Most of rats had mainly G2 grade tumors, and only 6 h-1 rat had muscle invasive G3 grade tumor. Representative images of white color light images and ALA-PDD at different times are shown in Fig. 1B and C. Although the area of fluorescence was small (Fig. 1D), red fluorescence was visible from 2 h after the oral administration of 5-ALA. The area of fluorescence (Fig. 1D) and the mean gray value (the average fluorescence intensity) (Fig. 1E) reached a peak level 4 h after 5-ALA administration. Red fluorescence was visible for up to 8 h after the oral administration of 5-ALA, while the area of fluorescence and the mean gray value decreased from 6 h after the oral administration of 5-ALA. Fig. 2 shows hematoxylin and eosin staining images, histopathological diagnosis, white color light images, and ALA-PDD (blue light) images 6 h after oral administration of 5-ALA in non-muscle-invasive and muscle-invasive bladder tumor lesions. Non-muscle-invasive bladder tumors were clearly visible by ALA-PDD 6 h after oral 5-ALA administration, whereas the fluorescence intensity on muscle-invasive, high grade G3, lesions (white arrowhead) in 6 h-1 rat was very weak. These findings suggest that although the optimal timing of the oral administration of 5-ALA could be 4 h before PDD, non-muscle-invasive bladder tumor lesions might be detected by ALA-PDD 2–8 h after administration in BBN-induced bladder tumor bearing rats.

3.2. 5-ALA and PpIX concentration after administration of 5-ALA in carcinogen-induced bladder cancer orthotopic rat model

We evaluated plasma 5-ALA, PpIX, and intratissue PpIX concentrations after oral 5-ALA administration in the BBN-induced bladder cancer orthotopic rat model. Plasma 5-ALA concentration (μM) remarkably

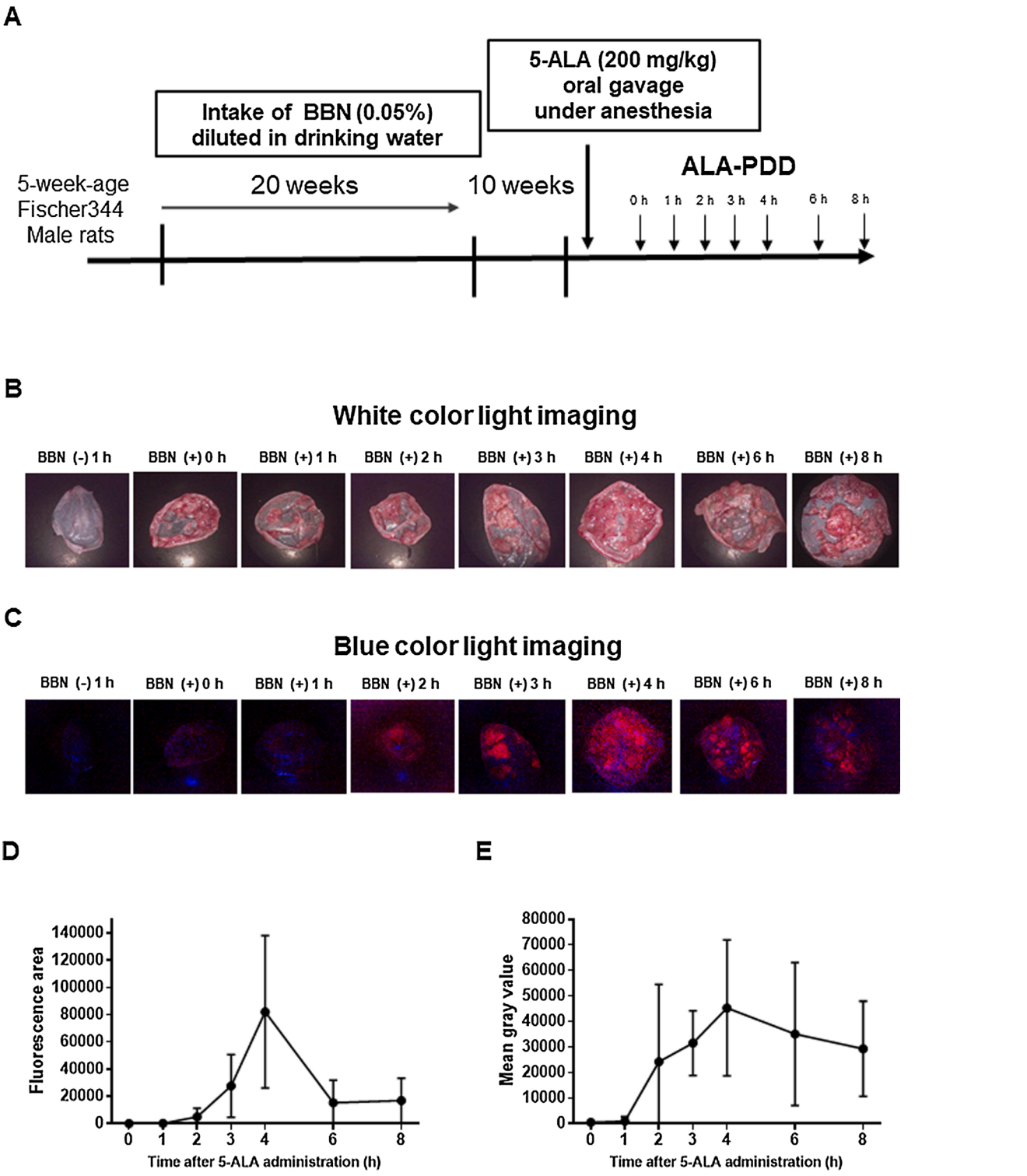

Fig. 1. Protocol of the animal study that investigated the duration of the photodynamic effect by oral administration of 5-aminolevulic acid (5-ALA) in a carcinogen-induced bladder cancer orthotopic rat model. The carcinogen-induced bladder cancer orthotopic rat model was established by the administration of N-butyl-N-(4-hydroxybutyl) nitrosamine for 20 weeks. 5-Aminolevulic acid hydrochloride (200 mg/kg) was orally administered (A). Representative images of photodynamic diagnosis using 5-ALA (ALA-PDD) (C) at different times corresponding to white color light images (A). The area of fluorescence (D) and mean gray value (the average of fluorescence intensity) (E) were analyzed using ImageJ software.

increased 1 h after the oral administration of 5-ALA (Fig. 3A). It decreased to around 100 μM 2 h after the administration of 5-ALA and remained at the same level 2–8 h after the administration. Plasma PplX concentration (nM) reached a peak concentration at 4 h and remained higher level for up to 8 h after the oral administration of 5-ALA (Fig. 3B). Intratissue PplX concentration (nmol/g tissue) also reached a peak concentration at 4 h and remained at the same level 8 h after the administration (Fig. 3C). When the intratissue PplX concentration was normalized by total tissue protein concentration, intratissue PplX concentration (nmol/g protein) remained at high levels 2–8 h after oral 5-

Table 1
Histopathological characteristics in BBN-induced bladder tumor orthotopic rat model.

Time after the administration of 5-ALA·HCl	Sample number	malignancy	pT stage	Grade	Concomitant CIS
–	negative control 1	no malignancy	–	–	–
–	negative control 2	no malignancy	–	–	–
0 h	1	urothelial carcinoma	a	2	–
	2	urothelial carcinoma	a	2 > 3	+
	3	urothelial carcinoma	2	2 > 3	+
	4	urothelial carcinoma	a	2 > 3	+
	5	urothelial carcinoma	a	2 > 3	–
	6	urothelial carcinoma	a	2 > 3	–
1 h	1	urothelial carcinoma	a	2	–
	2	urothelial carcinoma	a	2	–
	3	urothelial carcinoma	a	2 > 3	+
	4	urothelial carcinoma	a	2 > 3	+
	5	no malignancy	–	–	–
	6	urothelial carcinoma	1	2 > 3	+
2 h	1	urothelial carcinoma	a	2 > 3	+
	2	urothelial carcinoma	a	2	–
	3	urothelial carcinoma	a	2	–
	4	urothelial carcinoma	a	2 > 3	+
	5	urothelial carcinoma	a	2	–
	6	urothelial carcinoma	a	2 > 3	–
3 h	1	urothelial carcinoma	a	2 > 3	–
	2	urothelial carcinoma	a	2	–
	3	urothelial carcinoma	a	2 > 3	–
	4	urothelial carcinoma	a	2 > 3	+
	5	urothelial carcinoma	a	2	–
	6	urothelial carcinoma	a	2	–
4 h	1	urothelial carcinoma	a	2 > 3	+
	2	urothelial carcinoma	a	2	–
	3	urothelial carcinoma	a	2	–
	4	urothelial carcinoma	1	2 > 3	–
	5	urothelial carcinoma	1	2 > 3	–
	6	urothelial carcinoma	2	2 > 3	–
6 h	1	urothelial carcinoma	2	3 > 2	–
	2	urothelial carcinoma	a	2 > 3	–
	3	urothelial carcinoma	a	2 > 3	–
	4	urothelial carcinoma	a	2 > 3	–
	5	urothelial carcinoma	1	2 > 3	–
	6	urothelial carcinoma	a	2 > 3	+
8 h	1	urothelial carcinoma	a	2	–
	2	urothelial carcinoma	a	2 > 3	–
	3	urothelial carcinoma	a	2	–
	4	urothelial carcinoma	a	2 > 3	–
	5	urothelial carcinoma	a	2 > 3	–
	6	urothelial carcinoma	a	2	–

BBN; *N*-butyl-*N*-(4-hydroxybutyl) nitrosamine, 5-ALA·HCl; 5-aminolevulic acid hydrochloride, CIS; carcinoma *in situ*.

ALA administration (Fig. 3D).

3.3. 5-ALA-mediated PpIX accumulation in bladder cancer cell lines

To validate the findings in BBN-induced bladder tumor rat model, the fluorescence intensity of intracellular accumulated PpIX in three different phenotypes of bladder cancer cells after exposure to 5-ALA (1 mM) for different time points (0, 1, 2, 3, 4, 6, and 8 h) was analyzed by fluorescence microscopy (Fig. 4A, B). Accumulated PpIX in mitochondria of bladder cancer cells was visible 2 h after the administration of 5-ALA (Fig. 4C-E). The fluorescence intensity of PpIX reached a peak at 3 h in MGHU3 cells, whereas peak fluorescence intensities in UMUC3 and T24 cells were observed 4 h after the administration of 5-ALA (Fig. 4B). Next, to evaluate the sustainability of PpIX accumulation after the peak accumulation level in urothelial bladder cancer cells, we investigated PpIX accumulation at different time points (0, 1, 2, 3, and 4 h) after incubation with 5-ALA for 4 h; the medium was subsequently replaced with 5-ALA-free new medium (Fig. 5A).The fluorescence intensity remained high for 3 h and PpIX accumulation was visible even at 4 h after the removal of 5-ALA in UMUC3 cells (Fig. 5B, C). In contrast, the fluorescence intensities decreased after 1 h, and PpIX accumulation became unclear 3 h after the removal of 5-ALA in MGHU3 and T24 cells (Fig. 5B, D, E). These findings suggest that PpIX accumulation mediated by 5-ALA reaches a peak level 3–4 h after the administration of 5-ALA in bladder cancer cell lines as the same result as rat models. The PpIX remains accumulated for 2–4 h after peak accumulation in bladder cancer cells even if the culture medium does not contain 5-ALA.

3.4. PpIX accumulation is associated with the expression of ferrochelatase

We evaluated protein and mRNA expression of FECH in three phenotypes of urothelial bladder cancer cells. As shown in Fig. 6A, immunoblotting revealed that the protein expression level of FECH was lower in UMUC3 cells than in MGHU3 and T24 cells. Real-time PCR also revealed that the mRNA expression level of FECH was significantly lower in UMUC3 cells than in MGHU3 and T24 cells (Fig. 6B), suggesting that the lower expression level of FECH in UMUC3 cells was associated with longer duration of PpIX accumulation.

4. Discussion

5-ALA is a precursor of heme in the heme biosynthesis pathway, which is converted into endogenous fluorescent PpIX. This

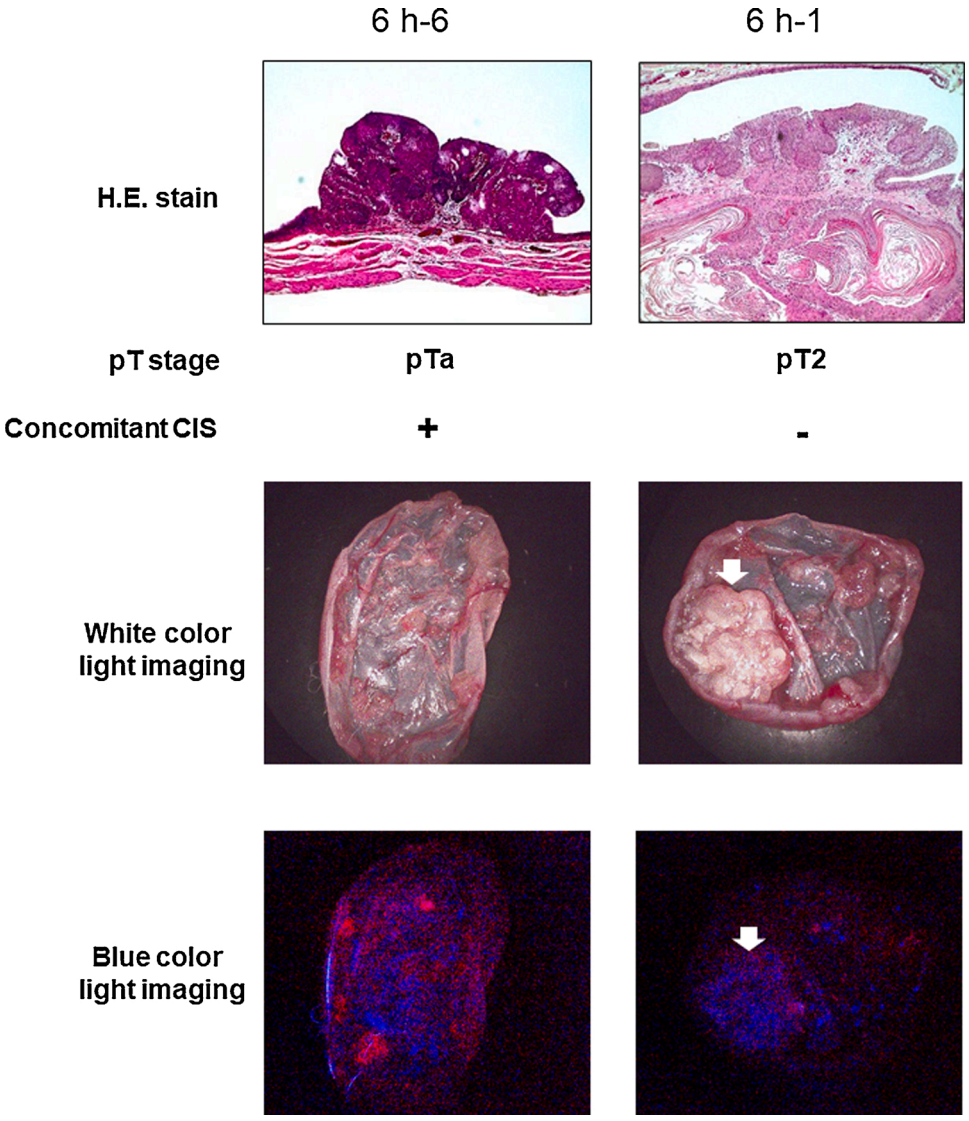

Fig. 2. Hematoxylin and eosin staining images, histopathological features, white color light images, and photodynamic diagnosis using 5-aminolevulic acid hydrochloride (5-ALA) (ALA-PDD) images taken 6 h after the oral administration of 5-ALA in non-muscle-invasive and muscle-invasive bladder cancer lesions. The white arrowhead indicates muscle-invasive bladder tumor in a N-butyl-N-(4-hydroxybutyl) nitrosamine (BBN)-induced bladder cancer orthotopic rat model.

bioconversion is catalyzed by FECH, which inserts ferrous iron into PpIX to produce heme. PpIX is preferentially accumulated in the mitochondria of cancer cells. Particularly, bladder cancer cells show 9- to 16-fold accumulation of PpIX compared to that in normal urothelial cells [10]. Intracellular PpIX is visible as red fluorescence at an excitation wavelength of approximately 400 nm and a peak emission wavelength of 635 nm [13]. This is the principal molecular mechanism underlying ALA-PDD. ALA-PDD is used for the detection of tumors during surgery in bladder [17,18] and brain tumors [24,25]. Oral administration of 5-ALA·HCl is recommended for 3 h (range, 2–4 h) before cystoscopy for bladder cancer and before anesthesia for brain tumors. However, there is insufficient evidence for the time duration of PDD fluorescence after oral administration of 5-ALA for detecting bladder cancer. In some cases, urologists might not be able to start ALA-PDD-assisted TURBT 2–4 h after the administration of 5-ALA. Yamamoto et al. reported that among a total of 76 patients who underwent ALA-PDD-assisted TURBT, 15 (20 %) received TURBT more than 4 h after oral 5-ALA administration [26]. In the present study, we evaluated the duration of the photodynamic effect after 5-ALA administration and confirmed whether the fluorescence in ALA-PDD could be detected when time had unexpectedly passed after the administration of 5-ALA. To the best of our knowledge, this is the first report to investigate the sustained fluorescence in PDD mediated by 5-ALA using a carcinogen-induced bladder tumor-bearing rat model and various phenotypes of bladder cancer cell lines.

Yamamoto et al. retrospectively investigated the diagnostic accuracy of ALA-PDD in 76 patients who underwent ALA-PDD-assisted TURBT for bladder tumors [26]. They showed that ALA-PDD could detect bladder tumors accurately in 15 patients with more than 4 h of 5-ALA exposure (306 ± 60 min) before ALA-PDD. Regarding the detection of brain tumors, Kaneko et al. demonstrated the maximum value of fluorescence intensity and a peak level of PpIX concentration in brain tumors 7–8 h after the oral administration of 5-ALA [27]. Moreover, Stummer et al. demonstrated that the average peak plasma concentration of PpIX was observed 7.8 h after the oral administration of 5-ALA·HCl (20 mg/kg) [28]. In contrast, our findings demonstrated that the maximum fluorescence intensity and fluorescence area were observed at 4 h after oral administration of 5-ALA in a BBN-induced rat model. Some lesions, especially MIBC lesion at 6 h after the administration of 5-ALA (Fig. 2), were false-negative in rats with more than 4 h exposure of 5-ALA. However, most of the non-muscle invasive lesions could be detected by ALA-PDD up to 8 h after the oral administration of 5-ALA. Additionally, plasma PpIX (nM) reached higher level at 4 h and intratumor

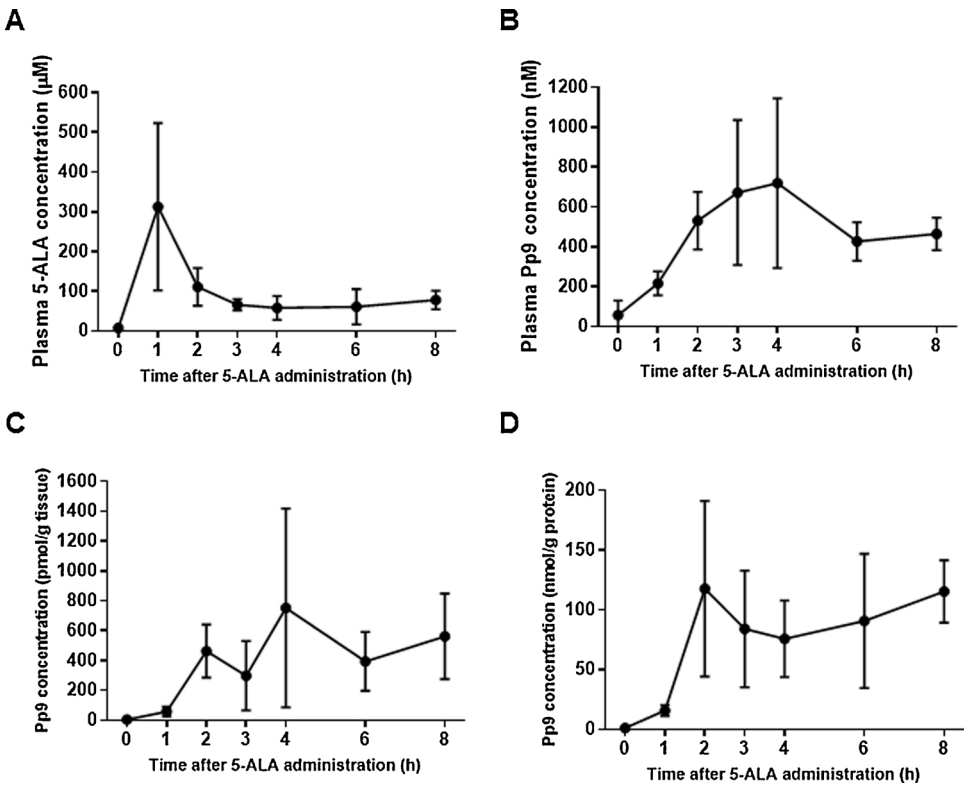

Fig. 3. Plasma 5-aminolevulic acid (5-ALA) and protoporphyrin IX (PpIX) concentration, and intratissue PpIX concentration at different time-points (0, 1, 2, 3, 4, 6, 8 h) after oral administration of 5-ALA in N-butyl-N-(4-hydroxybutyl) nitrosamine (BBN)-induced bladder cancer orthotopic rat model were analyzed by high-performance liquid chromatography (HPLC). (A) Plasma 5-ALA concentration (μM) was analyzed using 0.1 mL of plasma sample. (B) Plasma PpIX concentration (nM) was analyzed using 0.1 mL plasma sample. (C) Intratissue PpIX concentration (nmol/g tissue) was analyzed using 0.1 mL of homogenized tissue samples. (D) The data of intratissue PpIX concentration normalized by total tissue protein concentration (nmol/g protein).

PpIX concentration normalized by total tissue protein concentration (nmol/g protein) remained almost constant 2–8 h after the oral administration of 5-ALA. These findings suggested that it took at least 2 h for the exogenously administered 5-ALA to take into bladder tumor tissues and biosynthesize PpIX in the BBN-induced bladder tumor rat model. Therefore, the administration of 5-ALA 2 h before PDD is too early to detect bladder tumors. The biosynthesized PpIX remained accumulated at high levels in the bladder tumor tissue 8 h after oral administration of 5-ALA, suggesting ALA-PDD with more than 4 h of 5-ALA exposure could be feasible for detection of NMIBC. Webber et al. demonstrated that the time from oral 5-ALA administration to peak plasma PpIX levels was 8–12 h in humans [29]. Regarding the plasma concentration of 5-ALA, in the present study, the concentration (μM) reached a peak at 1 h and declined rapidly 2 h after the oral administration of 5-ALA. It is reported that the plasma concentration of 5-ALA was achieved 0.83 ± 0.2 h after oral administration of 5-ALA in humans [30]. These results suggest that there are no differences in the rate of pharmacokinetic uptake of 5-ALA after its oral administration between rats and humans. However, there could be a difference in the metabolism of the PpIX-heme biosynthetic pathway between rats and humans. Because no studies so far specifically investigated the differences of these metabolism in bladder tumors between rats and humans, clinical studies are needed to evaluate the time-dependent fluorescence intensity and plasma and intratissue PpIX concentrations after oral administration of 5-ALA in patients with bladder tumor.

To validate the findings in BBN-induced bladder tumor rat model, we used three different phenotypes of bladder cancer cell lines to evaluate time-dependent PpIX accumulation. Representative low-grade (MGHU3) and high-grade (UMUC3) human non-muscle-invasive bladder cancer cells [31,32] and representative muscle-invasive bladder cancer cells (T24) [33] were investigated. First, the maximum fluorescence intensity by ALA-PDD was observed 3–4 h after the administration of 5-ALA (Fig. 4). Subsequently, we investigated the PpIX accumulation after removal of 5-ALA because the cells were always exposure to 5-ALA on the culture medium. We showed that PpIX accumulation remained longer in non-muscle-invasive UMUC3 and MGHU3 cells than in muscle-invasive T24 cells; particularly, PpIX accumulation in UMUC3 cells remained for 4 h even if the culture medium did not contain 5-ALA. These findings might support the results of the carcinogen-induced bladder tumor orthotopic rat model wherein non-muscle-invasive lesions could be detected by ALA-PDD 6 h after the intake of 5-ALA, whereas particularly in 6 h-1 rat, which had muscle invasive high grade (G3) tumor, showed weak intensity (false-negative) by ALA-PDD during the same time (Fig. 2). These findings could be affected by differences in the metabolism of the PpIX-heme biosynthetic pathway and the tumor microenvironment between non-muscle-invasive and muscle-invasive bladder tumors. However, in this study, most of the BBN-induced bladder tumors were non-muscle invasive and G2 grade character tumors because BBN-induced bladder tumors in rats have papillary and non-muscle-invasive characteristics [20]. Thus, in this study, it was difficult to investigate the mechanism by which muscle invasive lesion could fall into being false-negative in cases with more than 4 h of 5-ALA exposure. Unfortunately, no studies so far specifically evaluated the differences in the metabolism of the PpIX-heme biosynthetic pathway between non-muscle and muscle invasive bladder tumors. Therefore, further studies are needed to investigate the differences in the sustainability of ALA-PDD and PpIX accumulation between non-muscle-invasive and muscle-invasive bladder tumors in both of human and rat specimens.

We showed that protein and mRNA expression levels of FECH were significantly lower in UMUC3 cells than in the other two cell lines. Downregulation of FECH has been shown to increase the fluorescence intensity and PpIX accumulation by inhibition of PpIX bioconversion to heme in bladder cancer, brain cancer, and breast cancer cells [11,12,34,35]. In this study, UMUC3 cells, which are non-muscle-invasive high--grade phenotypes, showed weak expression of FECH compared to that of MGHU3 and T24 cells, resulting in a longer photodynamic effect mediated by 5-ALA. In this study, we analyzed only 6 rats in each group and most of the BBN-induced bladder tumor rat models showed non-muscle invasive character. Therefore, we couldn't analyze the

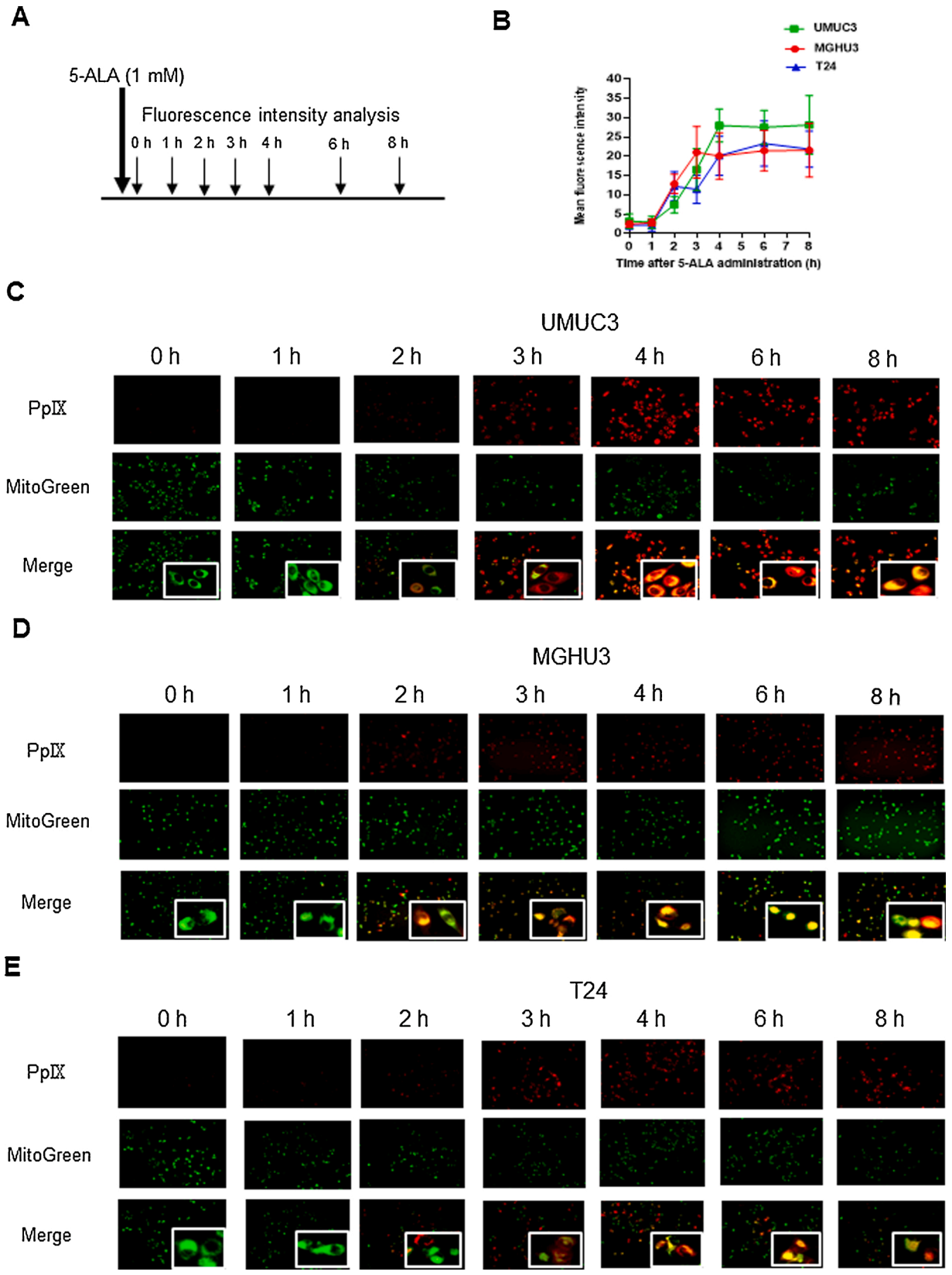

Fig. 4. Protocol of the analysis of time-dependent fluorescence intensity of accumulated protoporphyrin IX (PpIX) after the administration of 1 mM of 5-aminolevulic acid (5-ALA) (A). Fluorescence intensity was analyzed at different time-points (0, 1, 2, 3, 4, 6, and 8 h) after 5-ALA administration (B). Representative images of the accumulated PpIX and mitochondria in 3 phenotypes of bladder cancer cell lines, namely, UMUC3 (C), MGHU3 (D), and T24 (E), at different time-points (0, 1, 2, 3, 4, 6, and 8 h) after 5-ALA administration. Fluorescence images of PpIX were visualized under a fluorescence microscope with a specific filter (405 nm excitation, 630 nm emission). Mitochondria present in bladder cancer cells were labelled by green-fluorescence mitochondria dye (MitoGreen).

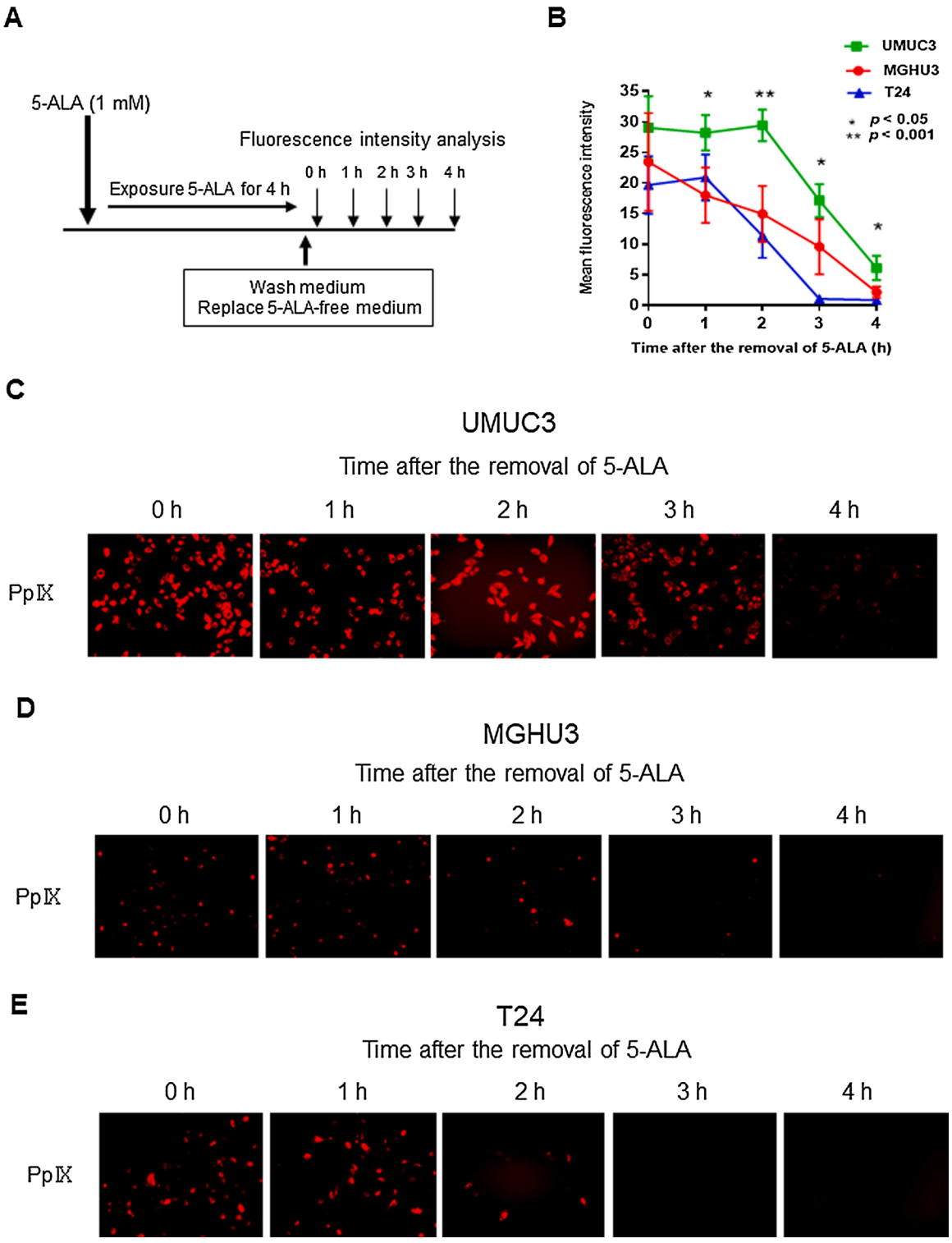

Fig. 5. Protocol of the analysis of time-dependent fluorescence intensity of protoporphyrinIX (PpIX) analyzed at different time-points (0, 1, 2, 3, and 4 h) after incubation with 5-ALA (1 mM) for 4 h and replaced with new ALA-free medium (A). Statistical analysis for fluorescence intensity was performed by student's *t*-test (Mean ± SEM. n = 5) (B). The representative images of accumulated PpIX in 3 phenotypes of bladder cancer cell lines including UMUC3 (C), MGHU3 (D), and T24 (E) at different time-points (0, 1, 2, 3, and 4 h) after the removal of 5-ALA. * $p < 0.05$, ** $p < 0.001$.

relation between the expression of FECH and muscle-invasion, and the sustainability of fluorescence *in vivo*. This is the important limitation in this study. We need to evaluate the relation between sustainability of fluorescence after the administration of 5-ALA and the expression of FECH using human samples during ALA-PDD-assisted TURBT.

In conclusion, this is the first report that investigated the sustained fluorescence in PDD and PpIX accumulation after 5-ALA administration using a BBN-induced bladder tumor orthotopic rat model. Our findings suggest that the optimal timing of the oral administration of 5-ALA could be 4 h before PDD for detection bladder tumors, while the principal aim of ALA-PDD could be achieved up to 8 h after oral administration of 5-ALA. Based on our findings, urologists might not be required to make

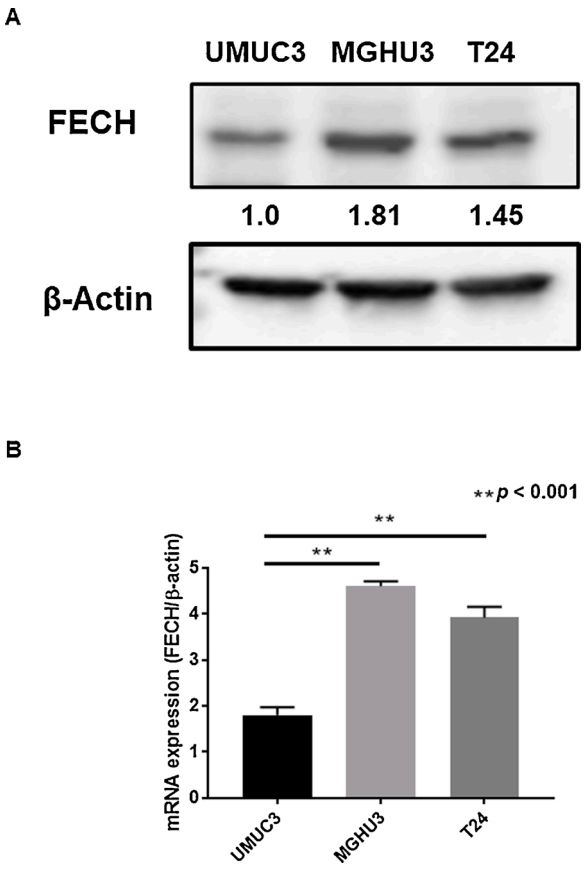

Fig. 6. Expression level of ferrochelatase in human urothelial bladder cancer cell lines, namely, UMUC3, MGHU3, and T24 cells. Protein expression levels were analyzed using western blot (A). The mRNA expression level was analyzed by quantitative real-time reverse transcription-polymerase chain reaction. In statistical analyses, mRNA levels were calculated using Student's *t*-test (Mean ± SEM. n = 3) (B). ** $p < 0.001$.

excess effort to start ALA-PDD-assisted transurethral resection of bladder tumor after the administration of 5-ALA.

Funding support

This article is a collaboration study with SBI Pharmaceuticals Co., Ltd. This study was partially funded by SBI Pharmaceuticals Co., Ltd., Tokyo, Japan.

Ethics statement

Animal examinations were performed according to the institutional guidelines approved by the Committee for Animal Experimentation of Nara Medical University, in accordance with the current regulations and standards of the Ministry of Health, Labor, and Welfare (Approval number: 12670).

Declaration of Competing Interest

Hara T, Ishi I, and Ota U are employed at SBI Pharmaceuticals Co., Ltd. The other authors declare no conflicts of interest.

Acknowledgments

The authors thank SBI Pharmaceuticals Co., Ltd. (Tokyo, Japan) for providing 5-aminolevulic acid hydrochloride in this study. We would like to thank Tomoya Nagano (SBI Pharmaceuticals Co., Ltd.) for their technical assistance in the animal study.

References

[1] S. Antoni, J. Ferlay, I. Soerjomataram, A. Znaor, A. Jemal, F. Bray, Bladder cancer incidence and mortality: a global overview and recent trends, Eur. Urol. 71 (2017) 96–108, https://doi.org/10.1016/j.eururo.2016.06.010.
[2] J. Miyazaki, H. Nishiyama, Epidemiology of urothelial carcinoma, Int. J. Urol. 24 (2017) 730–734, https://doi.org/10.1111/iju.13376.
[3] A. Kołodziej, W. Krajewski, M. Matuszewski, K. Tupikowski, Review of current optical diagnostic techniques for non-muscle-invasive bladder cancer, Cent. Eur. J. Urol. 69 (2016) 150–156, https://doi.org/10.5173/ceju.2016.780.
[4] N.M. Heney, Natural history of superficial bladder cancer. Prognostic features and long-term disease course, Urol. Clin. North Am. 19 (1992) 429–433.
[5] S.L. Woldu, A. Bagrodia, Y. Lotan, Guideline of guidelines: non-muscle-invasive bladder cancer, BJU Int. 119 (2017) 371–380, https://doi.org/10.1111/bju.13760.
[6] H.W. Herr, The value of a second transurethral resection in evaluating patients with bladder tumors, J. Urol. 162 (1999) 74–76, https://doi.org/10.1097/00005392-199907000-00018.
[7] H.E. Schwaibold, S. Sivalingam, F. May, R. Hartung, The value of a second transurethral resection for T1 bladder cancer, BJU Int. 97 (2006) 1199–1201, https://doi.org/10.1111/j.1464-410X.2006.06144.x.
[8] R. Gendy, W. Delprado, P. Brenner, A. Brooks, G. Coombes, P. Cozzi, P. Nash, M. I. Patel, Repeat transurethral resection for non-muscle-invasive bladder cancer: a contemporary series, BJU Int. 117 (2016) 54–59, https://doi.org/10.1111/bju.13265.
[9] K. Inoue, 5-Aminolevulinic acid-mediated photodynamic therapy for bladder cancer, Int. J. Urol. 24 (2017) 97–101, https://doi.org/10.1111/iju.13291.
[10] P. Steinbach, H. Weingandt, R. Baumgartner, M. Kriegmair, F. Hofstädter, R. Knüchel, Cellular fluorescence of the endogenous photosensitizer protoporphyrin IX following exposure to 5-aminolevulinic acid, Photochem. Photobiol. 62 (1995) 887–895, https://doi.org/10.1111/j.1751-1097.1995.tb09152.x.
[11] M. Miyake, M. Ishii, K. Kawashima, T. Kodama, K. Sugano, K. Fujimoto, Y. Hirao, siRNA-mediated knockdown of the heme synthesis and degradation pathways: modulation of treatment effect of 5-aminolevulinic acid-based photodynamic therapy in urothelial cancer cell lines, Photochem. Photobiol. 85 (2009) 1020–1027, https://doi.org/10.1111/j.1751-1097.2009.00543.x.
[12] Y. Nakai, Y. Tatsumi, M. Miyake, S. Anai, M. Kuwada, S. Onishi, Y. Chihara, N. Tanaka, Y. Hirao, K. Fujimoto, Expression of ferrochelatase has a strong correlation in protoporphyrin IX accumulation with photodynamic detection of bladder cancer, Photodiagn. Photodyn. Ther. 13 (2016) 225–232, https://doi.org/10.1016/j.pdpdt.2015.07.174.
[13] M. Miyake, Y. Nakai, S. Anai, Y. Tatsumi, M. Kuwada, S. Onishi, Y. Chihara, N. Tanaka, Y. Hirao, K. Fujimoto, Diagnostic approach for cancer cells in urine sediments by 5-aminolevulinic acid-based photodynamic detection in bladder cancer, Cancer Sci. 105 (2014) 616–622, https://doi.org/10.1111/cas.12393.
[14] M. Kriegmair, R. Baumgartner, R. Knuechel, P. Steinbach, A. Ehsan, W. Lumper, F. Hofstädter, A. Hofstetter, Fluorescence photodetection of neoplastic urothelial lesions following intravesical instillation of 5-aminolevulinic acid, Urology 44 (1994) 836–841, https://doi.org/10.1016/s0090-4295(94)80167-3.
[15] M. Babjuk, M. Burger, E. Compérat, P. Gontero, A.H. Mostafid, J. Palou, B.W. van Rhijn, M. Rouprêt, S.F. Shariat, R. Sylvester, R. Zigeuner, EAU Guideline, Non-muscle-invasive Bladder Cancer. 5. Diagnosis. 5.11. New Methods of Tumor Visualization, 5.14. Summary of Evidence and Guidelines for Transurethral Resection of the Bladder, Biopsies and Pathology Report, 2020. https://uroweb.org/guideline/non-muscle-invasive-bladder-cancer/#5.
[16] H. Matsuyama, M. Nakagawa, J. Inoguchi, T. Tsuzuki, K. Fujimoto, et al., Clinical Guideline for Bladder Cancer, 3rd edition, Igakutosho-Shuppan, Ltd, Tokyo, 2019 (In Japanese.).
[17] K. Inoue, S. Anai, K. Fujimoto, Y. Hirao, H. Furuse, F. Kai, S. Ozono, T. Hara, H. Matsuyama, M. Oyama, M. Ueno, H. Fukuhara, M. Narukawa, T. Shuin, Oral 5-aminolevulinic acid mediated photodynamic diagnosis using fluorescence cystoscopy for non-muscle-invasive bladder cancer: A randomized, double-blind, multicentre phase II/III study, Photodiagn. Photodyn. Ther. 12 (2015) 193–200, https://doi.org/10.1016/j.pdpdt.2015.03.008.
[18] Y. Nakai, K. Inoue, T. Tsuzuki, T. Shimamoto, T. Shuin, K. Nagao, H. Matsuyama, M. Oyama, H. Furuse, S. Ozono, M. Miyake, K. Fujimoto, Oral 5-aminolevulinic acid-mediated photodynamic diagnosis using fluorescence cystoscopy for non-muscle-invasive bladder cancer: a multicenter phase III study, Int. J. Urol. 25 (2018) 723–729, https://doi.org/10.1111/iju.13718.
[19] E. Okajima, A. Denda, S. Ozono, M. Takahama, H. Akai, Y. Sasaki, W. Kitayama, K. Wakabayashi, Y. Konishi, Chemopreventive effects of nimesulide, a selective cyclooxygenase-2 inhibitor, on the development of rat urinary bladder carcinomas initiated by N-butyl-N-(4-hydroxybutyl) nitrosamine, Cancer Res. 58 (1998) 3028–3031.
[20] C. Vasconcelos-Nóbrega, A. Colaço, C. Lopes, P.A. Oliveira, Review: BBN as an urothelial carcinogen, In Vivo (Brooklyn) 26 (2012) 727–739.
[21] J. Schindelin, I. Arganda-Carreras, E. Frise, V. Kaynig, M. Longair, T. Pietzsch, S. Preibisch, C. Rueden, S. Saalfeld, B. Schmid, J.Y. Tinevez, D.J. White, V. Hartenstein, K. Eliceiri, P. Tomancak, A. Cardona, Fiji: an open-source platform for biological-image analysis, Nat. Methods 9 (2012) 676–682, https://doi.org/10.1038/nmeth.2019.
[22] U. Ota, H. Fukuhara, M. Ishizuka, F. Abe, C. Kawada, K. Tamura, T. Tanaka, K. Inoue, S.I. Ogura, T. Shuin, Plasma protoporphyrin IX following administration

of 5-aminolevulinic acid as a potential tumor marker, Mol. Clin. Oncol. 3 (2015) 797–801, https://doi.org/10.3892/mco.2015.549.
[23] T. Osaki, I. Yokoe, Y. Sunden, U. Ota, T. Ichikawa, H. Imazato, T. Ishii, K. Takahashi, M. Ishizuka, T. Tanaka, L. Li, M. Yamashita, Y. Murahata, T. Tsuka, K. Azuma, N. Ito, T. Imagawa, Y. Okamoto, Efficacy of 5-aminolevulinic acid in photodynamic detection and photodynamic therapy in veterinary medicine, Cancers (Basel). 11 (2019) 495, https://doi.org/10.3390/cancers11040495.
[24] W. Stummer, U. Pichlmeier, T. Meinel, O.D. Wiestler, F. Zanella, H.J. Reulen, ALA-Glioma Study Group, Fluorescence-guided surgery with 5-aminolevulinic acid for resection of malignant glioma: a randomised controlled multicentre phase III trial, Lancet Oncol. 7 (2006) 392–401, https://doi.org/10.1016/S1470-2045(06)70665-9.
[25] U. Pichlmeier, A. Bink, G. Schackert, W. Stummer, ALA Glioma Study Group, Resection and survival in glioblastoma multiforme: an RTOG recursive partitioning analysis of ALA study patients, Neuro. Oncol. 10 (2008) 1025–1034, https://doi.org/10.1215/15228517-2008-052.
[26] S. Yamamoto, H. Fukuhara, T. Karashima, K. Inoue, Real-world experience with 5-aminolevulinic acid for the photodynamic diagnosis of bladder cancer: diagnostic accuracy and safety, Photodiagn. Photodyn. Ther. 32 (2020) 101999, https://doi.org/10.1016/j.pdpdt.2020.101999.
[27] S. Kaneko, E. Suero Molina, C. Ewelt, N. Warneke, W. Stummer, Fluorescence-based measurement of real-time kinetics of protoporphyrin IX after 5-aminolevulinic acid administration in human in situ malignant gliomas, Neurosurgery 85 (2019) E739–E746, https://doi.org/10.1093/neuros/nyz129.
[28] W. Stummer, H. Stepp, O.D. Wiestler, U. Pichlmeier, Randomized, prospective double-blinded study comparing 3 different doses of 5-aminolevulinic acid for fluorescence-guided resections of malignant gliomas, Neurosurgery. 81 (2017) 230–239, https://doi.org/10.1093/neuros/nyx074.
[29] J. Webber, D. Kessel, D. Fromm, Plasma levels of protoporphyrin IX in humans after oral administration of 5-aminolevulinic acid, J. Photochem. Photobiol. B 37 (1997) 151–153, https://doi.org/10.1016/s1011-1344(96)07348-4.
[30] J.T. Dalton, C.R. Yates, D. Yin, A. Straughn, S.L. Marcus, A.L. Golub, M.C. Meyer, Clinical pharmacokinetics of 5-aminolevulinic acid in healthy volunteers and patients at high risk for recurrent bladder cancer, J. Pharmacol. Exp. Ther. 301 (2002) 507–512, https://doi.org/10.1124/jpet.301.2.507.
[31] B.A. Hadaschik, K. Zhang, A.I. So, L. Fazli, W. Jia, J.C. Bell, M.E. Gleave, P. S. Rennie, Oncolytic vesicular stomatitis viruses are potent agents for intravesical treatment of high-risk bladder cancer, Cancer Res. 68 (2008) 4506–4510, https://doi.org/10.1158/0008-5472.CAN-08-0238.
[32] D. Huebner, C. Rieger, R. Bergmann, M. Ullrich, S. Meister, M. Toma, R. Wiedemuth, A. Temme, V. Novotny, M.P. Wirth, M. Bachmann, J. Pietzsch, S. Fuessel, An orthotopic xenograft model for high-risk non-muscle invasive bladder cancer in mice: influence of mouse strain, tumor cell count, dwell time and bladder pretreatment, BMC Cancer 17 (2017) 790, https://doi.org/10.1186/s12885-017-3778-3.
[33] S. Ramakrishnan, W. Huss, B. Foster, J. Ohm, J. Wang, G. Azabdaftari, K.H. Eng, A. Woloszynska-Read, Transcriptional changes associated with *in vivo* growth of muscle-invasive bladder cancer cell lines in nude mice, Am. J. Clin. Exp. Urol. 6 (2018) 138–148.
[34] L. Teng, M. Nakada, S.G. Zhao, Y. Endo, N. Furuyama, E. Nambu, I.V. Pyko, Y. Hayashi, J.I. Hamada, Silencing of ferrochelatase enhances 5-aminolevulinic acid-based fluorescence and photodynamic therapy efficacy, Br. J. Cancer 104 (2011) 798–807, https://doi.org/10.1038/bjc.2011.12.
[35] P. Palasuberniam, D. Kraus, M. Mansi, A. Braun, R. Howley, K.A. Myers, B. Chen, Ferrochelatase deficiency abrogated the enhancement of aminolevulinic acid-mediated protoporphyrin IX by iron chelator deferoxamine, Photochem. Photobiol. 95 (2019) 1052–1059, https://doi.org/10.1111/php.13091.